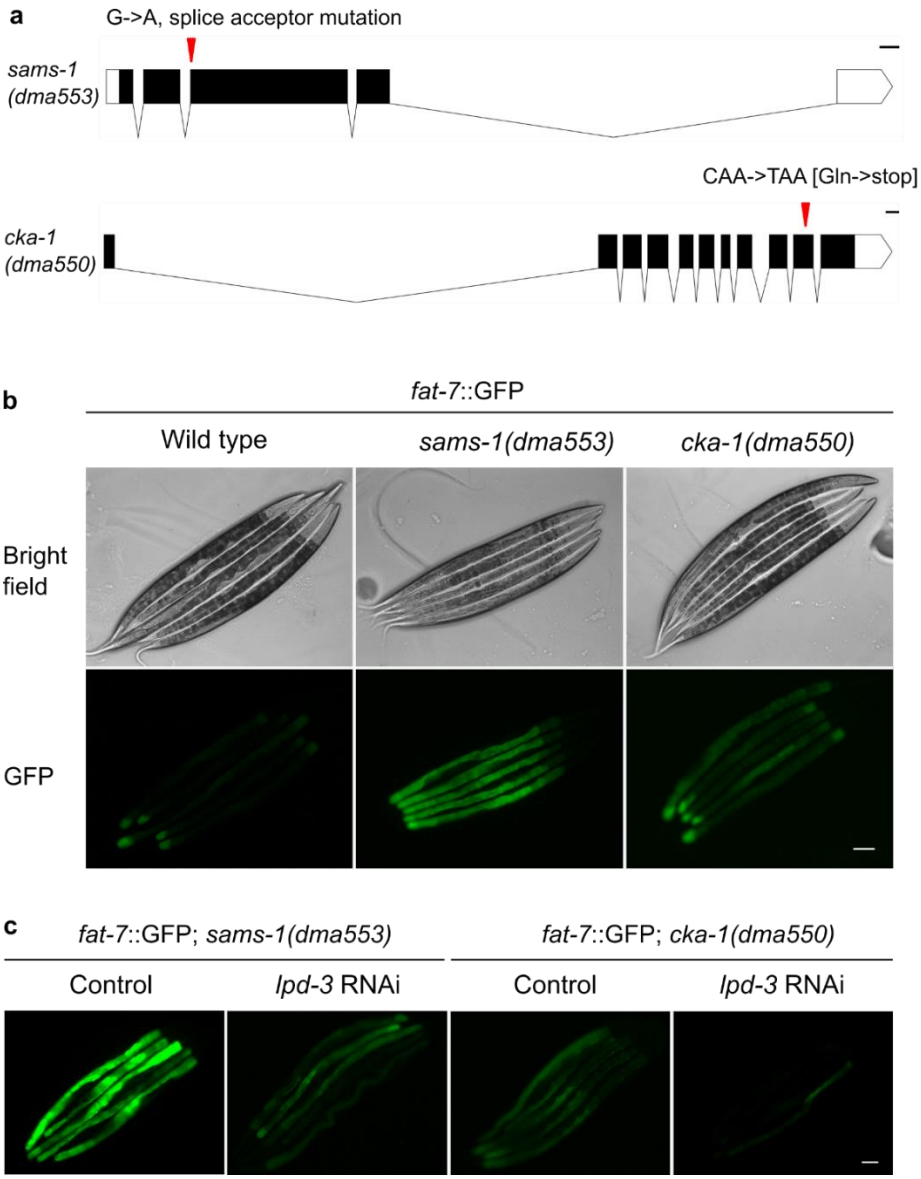

Supplementary Figure 1. Genetic identification of *cka-1* and *sams-1* in regulating *fat-7*::GFP. a, Gene diagrams showing *sams-1*(*dma553*) and *cka-1*(*dma550*) that cause a splice acceptor mutation and a premature stop codon mutation, respectively, identified by WGS. **b**, Representative bright-field and epifluorescence images showing activation of *fat-7*::GFP by *sams-1*(*dma553*) and *cka-1*(*dma550*). Both mutations were isolated from EMS screens and outcrossed at least 5 times, segregating with *fat-7*::GFP

activation phenotypes. **c**, Representative epifluorescence images showing that RNAi against *lpd-3* attenuated activation of *fat-7*::GFP by *sams-1*(*dma553*) or *cka-1*(*dma550*). Scale bar: 50 µm.

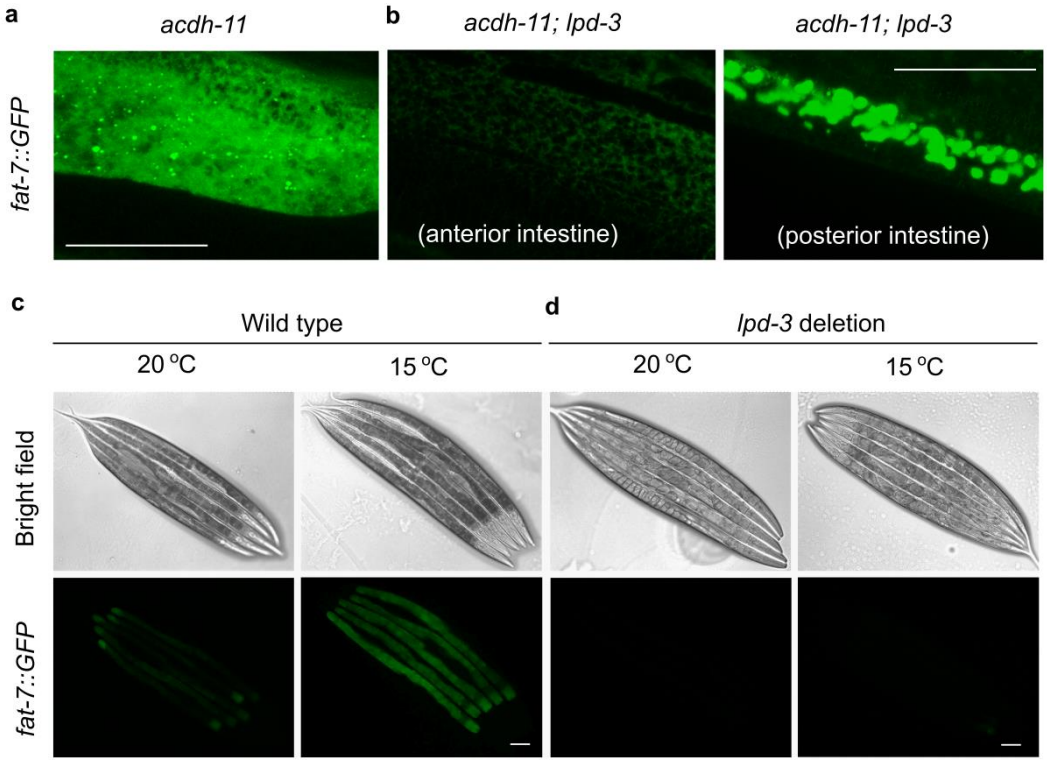

Supplementary Figure 2. *lpd-3* suppresses *acdh-11* or hypothermia-induced *fat-7*::GFP. a, Confocal fluorescence image (Z-stack) showing *fat-7*::GFP in *acdh-11(n5857)* mutants. **b**, Confocal fluorescence images showing *lpd-3(ok2138)* deletion mutation suppresses *fat-7*::GFP in *acdh-11(n5857)* mutants, more prominently in the anterior than posterior intestine. **c**, Bright field and epifluorescence images showing up-regulation of *fat-7*::GFP by hypothermia (15 °C 24 hrs). **d**, Bright field and epifluorescence images showing up-regulation of *fat-7*::GFP by hypothermia (15 °C 24 hrs) is blocked in *lpd-3(ok2138)* deletion mutants. Scale bar: 50 µm.

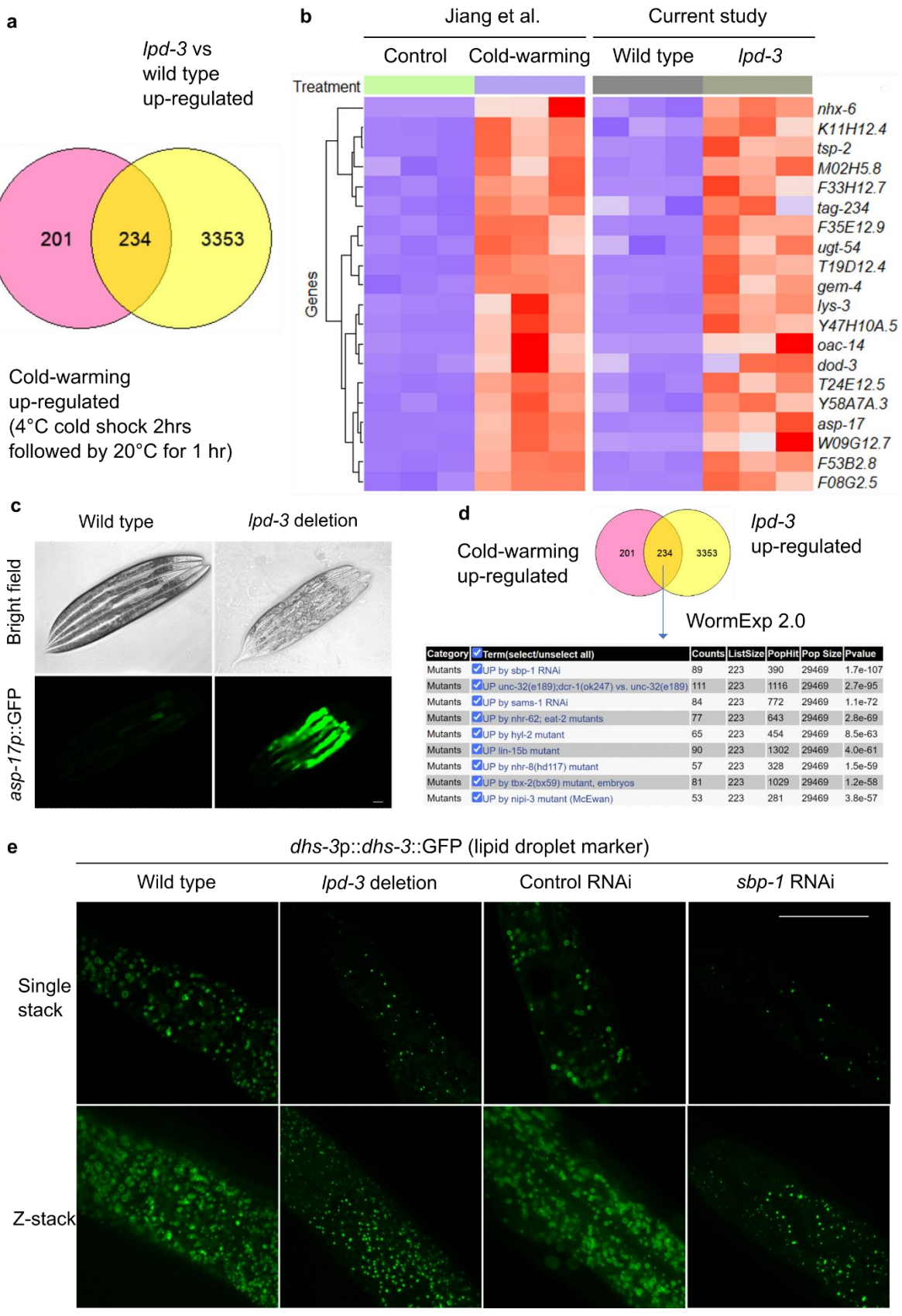
a
lpd-3 vs
wild type
up-regulated
201
234
3353
Cold-warming
up-regulated
(4°C cold shock 2hrs
followed by 20°C for 1 hr)
b
Jiang et al.
Current study
Control
Cold-warming
Wild type
lpd-3
Treatment
Genes
nhx-6
K11H12.4
tsp-2
M02H5.8
F33H12.7
tag-234
F35E12.9
ugt-54
T19D12.4
gem-4
lys-3
Y47H10A.5
oac-14
dod-3
T24E12.5
Y58A7A.3
asp-17
W09G12.7
F53B2.8
F08G2.5
c
Wild type
lpd-3 deletion
Bright field
asp-17p::GFP
d
Cold-warming
up-regulated
201
234
3353
lpd-3
up-regulated
WormExp 2.0
Category
Term(select/unselect all)
Counts
ListSize
PopHit
Pop Size
Pvalue
Mutants
UP by sbp-1 RNAi
89
223
390
29469
1.7e-107
Mutants
UP unc-32(e189);dcr-1(ok247) vs. unc-32(e189)
111
223
1116
29469
2.7e-95
Mutants
UP by sams-1 RNAi
84
223
772
29469
1.1e-72
Mutants
UP by nhr-62; eat-2 mutants
77
223
643
29469
2.8e-69
Mutants
UP by hyl-2 mutant
65
223
454
29469
8.5e-63
Mutants
UP lin-15b mutant
90
223
1302
29469
4.0e-61
Mutants
UP by nhr-8(hd117) mutant
57
223
328
29469
1.5e-59
Mutants
UP by tbx-2(bx59) mutant, embryos
81
223
1029
29469
1.2e-58
Mutants
UP by nipi-3 mutant (McEwan)
53
223
281
29469
3.8e-57
e
dhs-3p::dhs-3::GFP (lipid droplet marker)
Wild type
lpd-3 deletion
Control RNAi
sbp-1 RNAi
Single
stack
Z-stack

Supplementary Figure 3. RNAseq reveals genes commonly regulated by LPD-3, cold stress and SBP-1. a, Venn diagram showing commonly regulated genes by both *lpd-3(ok2138)* and cold stress. **b**, Heat map showing the top 30 regulated genes by *lpd-3(ok2138)* that are also regulated by cold stress. **c**, Bright field and epifluorescence images showing constitutive up-regulation of *asp-17p::*GFP in *lpd-3(ok2138)* mutants. Scale bar: 50 µm. **d**, WormExp (https://wormexp.zoologie.uni-kiel.de/wormexp/) analysis of *lpd-3* and cold-commonly regulated genes showing they are most similar to the gene set regulated by RNAi against *sbp-1*. *P* values were calculated by the program EASE based on the Fisher Exact test by the WormExp webpage. **e**, Representative confocal fluorescence images (Single stack, above; Z-stack, below) showing that both *lpd-3(ok2138)* and *sbp-1* RNAi can cause fewer in numbers and smaller in size of lipid droplet makers *dhs-3*p::*dhs-3*::GFP. Scale bar: 50 µm.

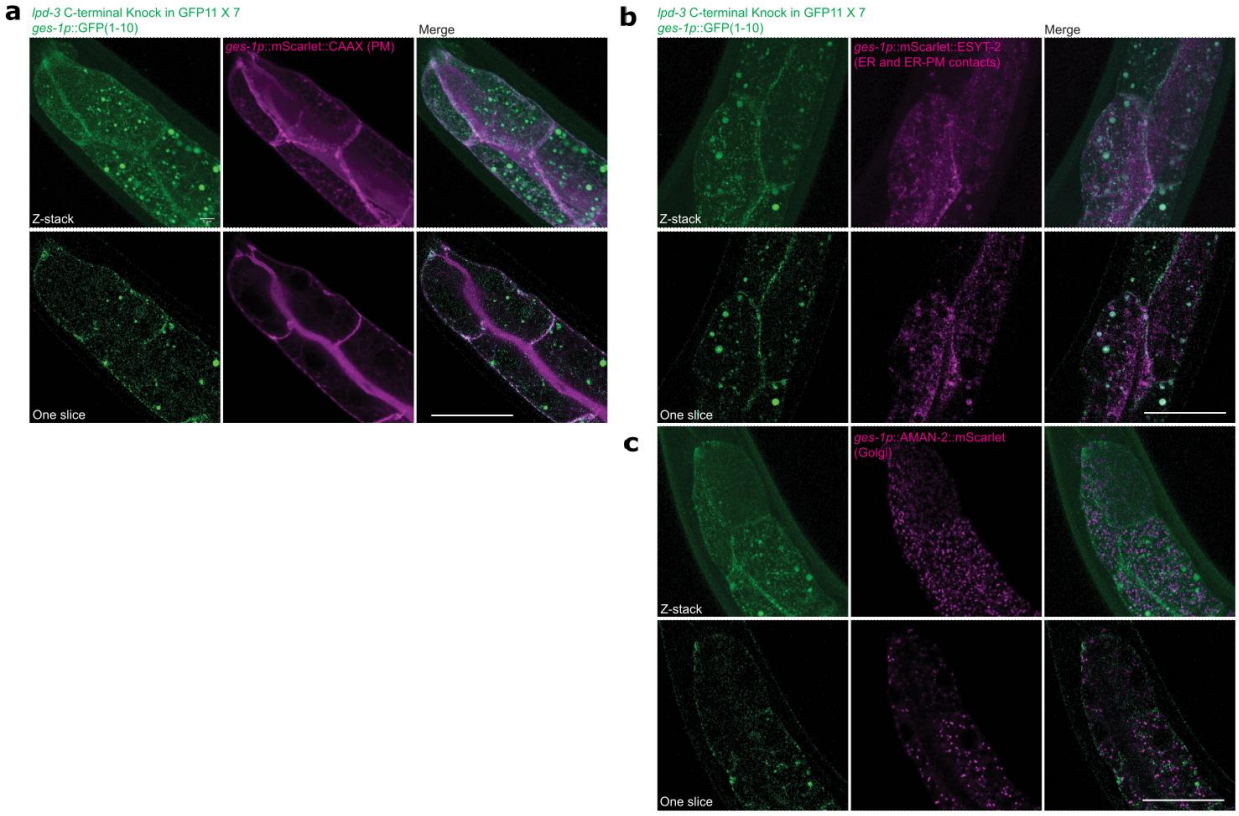

Supplementary Figure 4. Endogenous LPD-3 localizes to ER-PM membrane contact sites. a, Representative confocal fluorescence images showing endogenous LPD-3::GFP (generated by CRISPR/Cas9-mediated knock-in of 7xGFP11 and 7xGFP1-10 complementation) in apposition with mScarlet::CAAX(PM). **b**, Representative confocal fluorescence images showing endogenous LPD-3::GFP (generated by CRISPR/Cas9-mediated knock-in of GFP11 and 7xGFP1-10 complementation) in apposition with mScarlet::ESYT-2, a marker for ER-PM junctions. **c**, Representative confocal fluorescence images showing endogenous LPD-3::GFP (generated by CRISPR/Cas9-mediated knock-in of GFP11 and 7xGFP1-10 complementation) in apposition with AMAN-2::mScarlet, a Golgi marker. Scale bar, 50 μm.

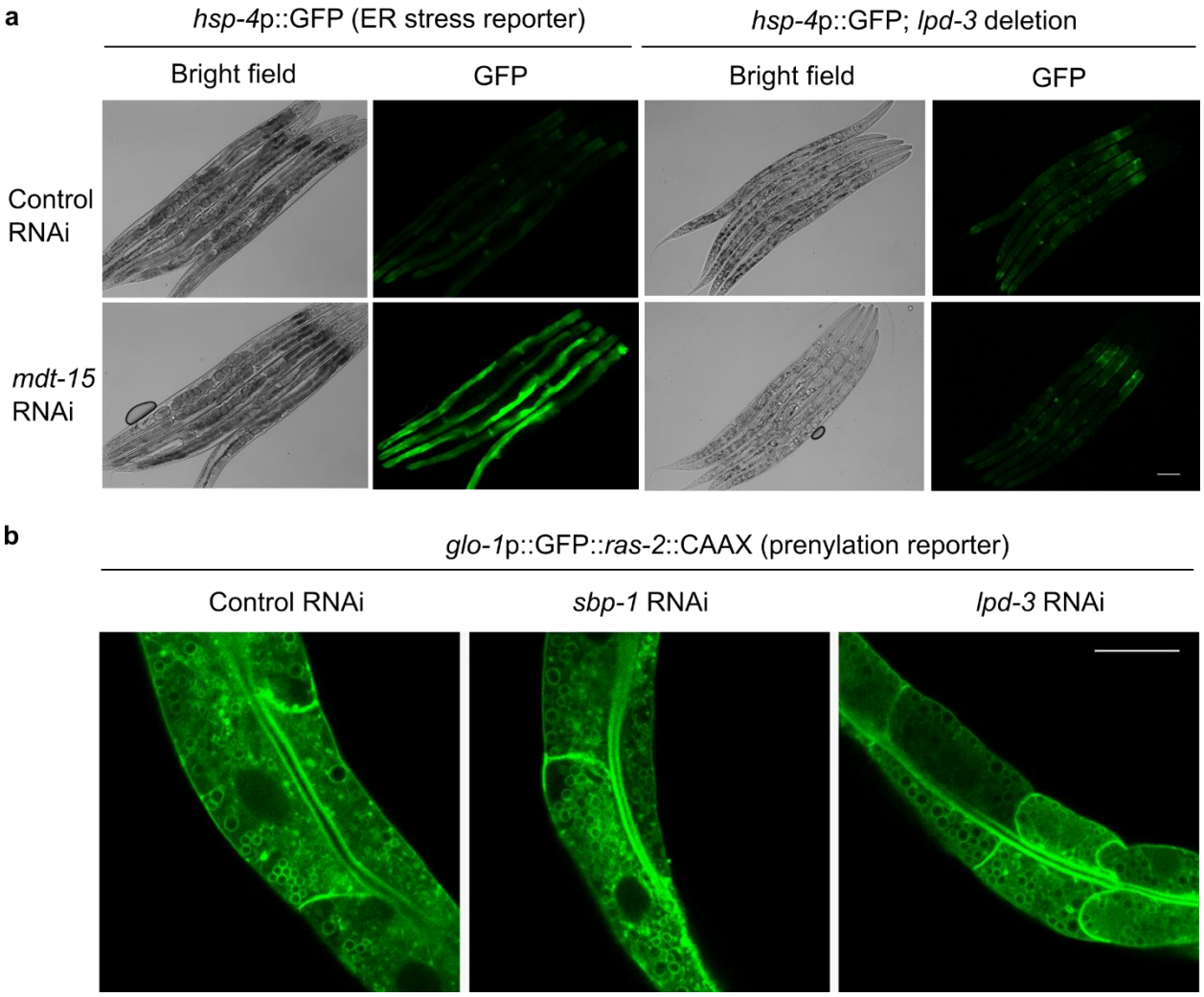

Supplementary Figure 5. Additional phenotypes of *lpd-3* mutants. a, Representative epifluorescence images showing activation of the *hsp-4*p::GFP ER stress reporter by RNAi against *mdt-15* in wild type but not *lpd-3(ok2138)* mutants. *mdt-15* RNAi activates *hsp-4*p::GFP because of reduced desaturase gene expression and excessive acyl chain saturation of ER membrane lipids[47]. **b,** Representative confocal fluorescence images showing largely normal intestinal PM morphology and PM-targeted trafficking of the prenylation reporter *glo-1*p::GFP::*ras-2*::CAAX in *sbp-1* or *lpd-3* RNAi-treated animals. Scale bar: 50 µm.

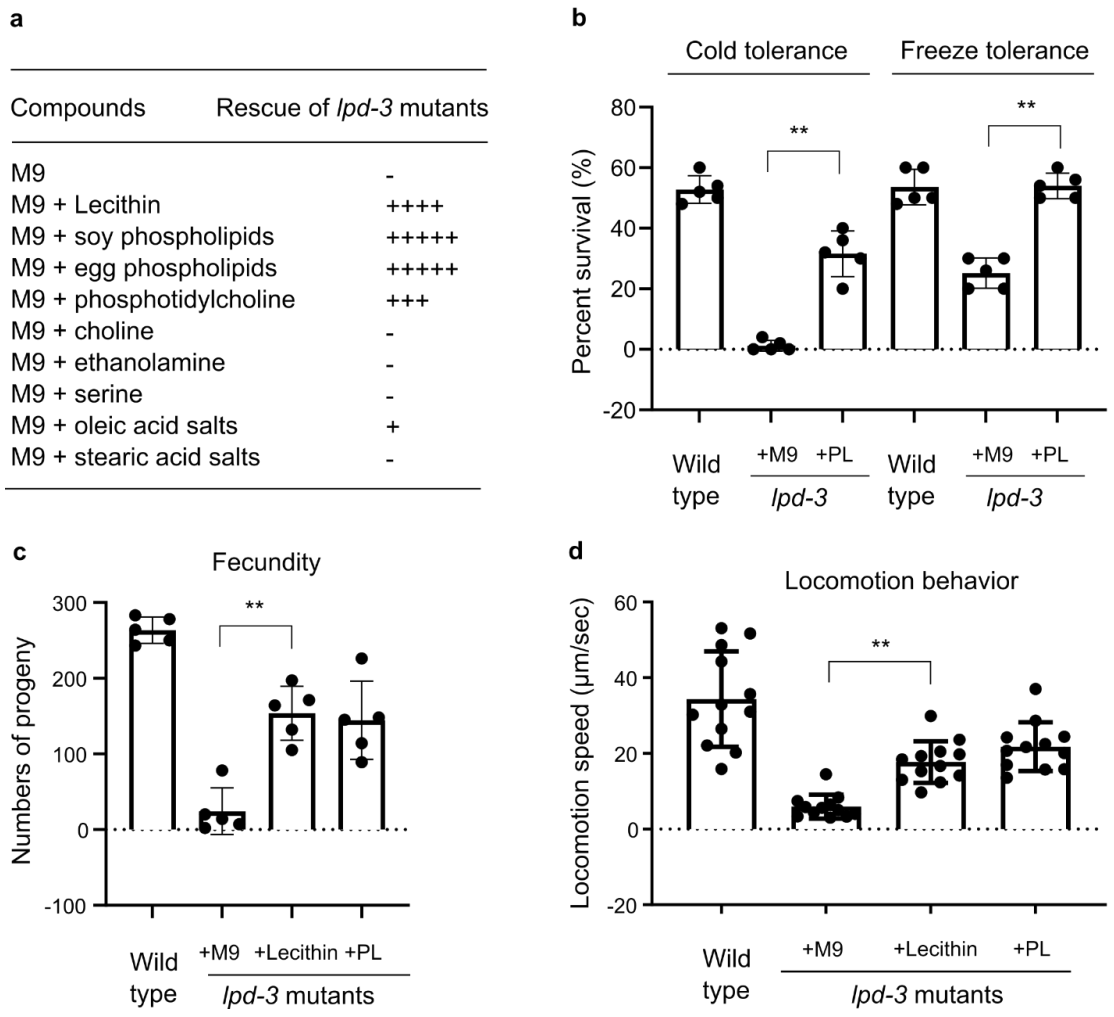

Supplementary Figure 6. Phospholipid/Lecithin rescue of various *lpd-3* mutant phenotypes. a, Table summary for the degrees of rescue (indicated by the numbers of + sign) of developmental delay in *lpd-3* mutants by Lecithin, phospholipids derived from soy or egg, or various other phospholipid constituent compounds. **b**, Quantification of percent survival of wild type or *lpd-3* mutants, and rescue by soy phospholipid (PL), in the cold or freezing tolerance assays. Values are means ± S.D with $^{**}P < 0.01$ (N = 5 independent experiments, one-way ANOVA followed by multiple two-sided unpaired t-tests). **c**, Quantification of fecundity (numbers of progeny per hermaphrodite) of wild type or *lpd-3* mutants, and rescue by soy phospholipid (PL) or Lecithin. Values are means ± S.D with $^{**}P < 0.01$ (N = 5 independent experiments, one-way ANOVA followed by multiple two-sided unpaired t-tests). **d**, Quantification of locomotion behavior (average speed of young adult hermaphrodite) of wild type or *lpd-3* mutants, and

rescue by soy phospholipid (PL) or Lecithin. Values are means ± S.D with $^{**}P < 0.01$ (N = 12 animals per group, one-way ANOVA followed by multiple two-sided unpaired t-tests). Source data are provided as a Source Data file.

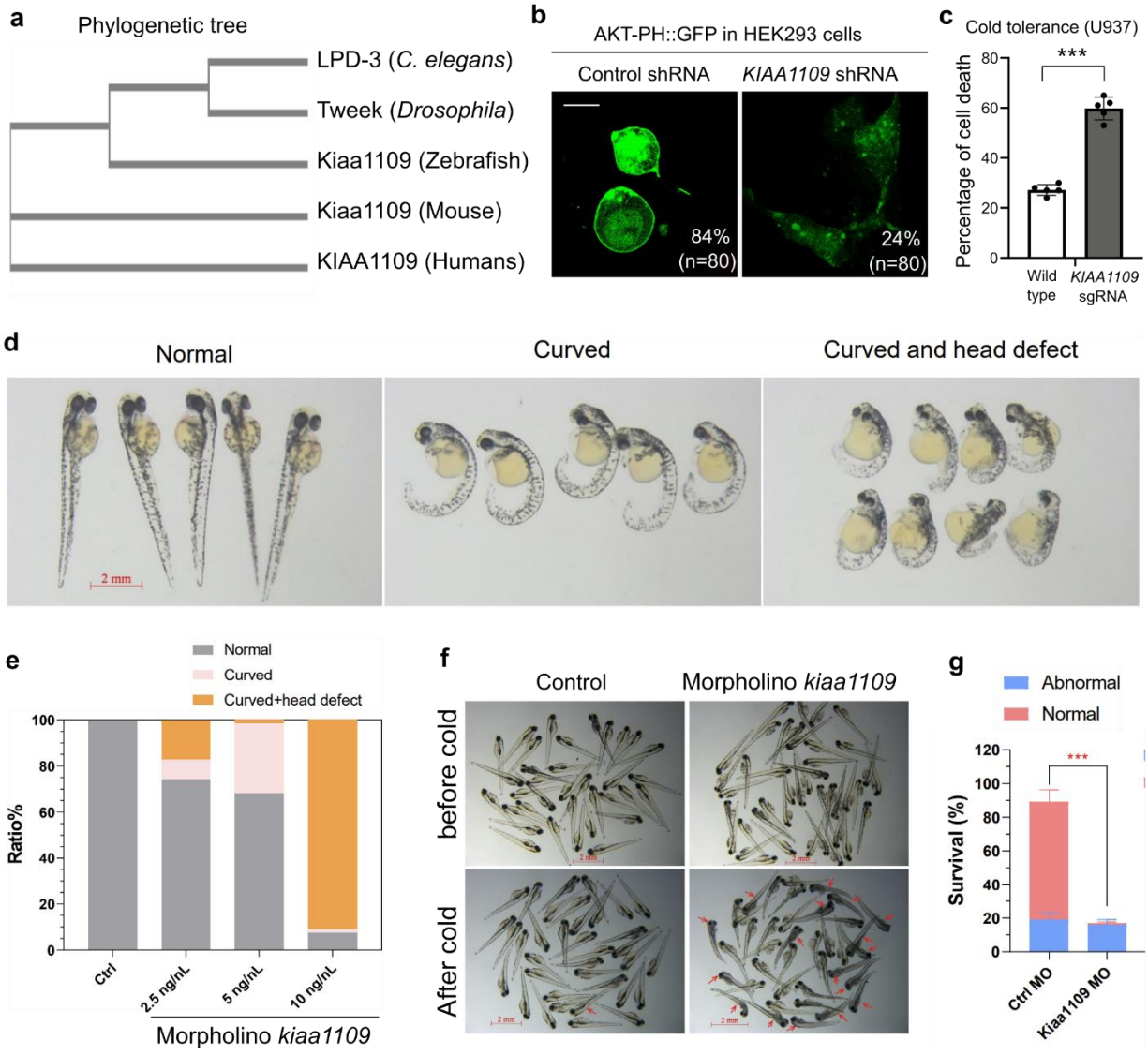

Supplementary Figure 7. Evidence for conserved roles of LPD-3 protein families in lipid trafficking and cold tolerance. a, Clustal Omega-generated phylogenetic tree of the LPD-3 protein family from major metazoan species (*C. elegans*, *Drosophila*, Zebrafish, mouse and humans). **b**, Representative

confocal fluorescence imaging of AKT-PH::GFP (PIP3 binding) in HEK293 cells co-transfected with the AKT-PH::GFP and shRNA (control or *KIAA1109* with 73% knockdown efficiency, SIGMA) plasmids, showing reduced plasma membrane localization of AKT-PH::GFP by shRNA against *KIAA1109.* Percentages of cells with normal membrane-localized fluorescent signals were noted for shRNA control and sh-*KIAA1109.* Scale bar: 10 μm. **c**, Percentage of cell death after cold shock (4 ^{o}C for 20 hrs) in wild type and *KIAA1109* KO cells generated by CRISPR/Cas9. Values are means ± S.D with ***, $P < 0.001$; N = 5 independent experiments (n > 400 cells analyzed by SYTOX Green for each experiment). **d**, Representative images of zebrafish embryos showing various morphological phenotypes caused by morpholino against *kiaa1109.* **e**, Quantification of the various morphological phenotypes caused by morpholino against *kiaa1109.* **f**, Representative images of zebrafish embryos showing a phenotype of reduced cell survival caused by morpholino against *kiaa1109.* **g**, Quantification of reduced cell survival caused by morpholino against *kiaa1109.* Values are means ± S.D with ***, $P < 0.001$; N = 6 independent experiments (n > 30 fish for each experiment). Source data are provided as a Source Data file.